IJCRT.ORG ISSN : 2320-2882

INTERNATIONAL JOURNAL OF CREATIVE RESEARCH THOUGHTS (IJCRT)

An International Open Access, Peer-reviewed, Refereed Journal

PERFORMANCE ENHANCEMENT OF INDUCTION MOTOR DRIVE USING SPRS WITH CURRENT CONTROLLED PWMVSI AND BUCK-BOOST CHOPPER

[1] [2] [3]
Sita Ram Bhardwaj, O. P. Rahi, Veena Sharma

[1] [2] [3]
Assistant Professor, Associate Professor, Associate Professor

[1]
Electrical Engineering Department,

[1]
Govt. Hydro Engineering College Bandla, Bilaspur HP, India

Abstract: The pulse width modulated voltage source inverters (PWMVSI) control the active and reactive power using voltage and current control techniques. The PWMVSI with chopper controller allows the reactive power and speed control simultaneously and hence achieves the decoupled control of induction motor drive. This paper presents the analysis of slip power recovery scheme (SPRS) based slip ring induction motor drive (SRIMD) employing buck-boost chopper and PWMVSI with current control technique. The objective of current control technique is to decrease the reactive power consumption of inverter from the supply, which in turn reduces the total harmonic distortion (THD) of supply current and improves the power factor and efficiency of SRIMD. The simulation model of *2 hp* motor has been developed in the MATLAB 2013a to analyze the performance characteristics of SRIMD. The simulation results have shown that the SPRS using buck-boost chopper and PWMVSI with current control technique have considerable reduction in reactive power consumption of inverter resulting in better THD of supply current, power factor, and efficiency of SRIMD compared to SPRS without chopper.

Index Terms - Component, Buck-boost chopper, inverter; induction motor drive, slip power recovery scheme, wound rotor induction motor.

I. INTRODUCTION

Speed control of induction motor has a vital attribute for variable speed drive (VSD) applications. The utilization of SRIMDs are rising speedily for VSD applications as a consequences of low maintenance, simple control of slip power from the slip rings, lesser cost, rugged design, and direct connection to alternating current (AC) supply. In the past, the mechanically controlled rotor resistance method was utilized to control the speed of slip ring induction motors (SRIMs) which produces power loss in the rotor resistance causing the decrease in efficiency of SRIM. The extension in the power electronic technology has played a important role to develop the slip power recovery scheme (SPRS) for recovering the slip power from the rotor circuit and feeding it back to the supply, therefore, increases the efficiency (Lavi A and Polge R. J, Kumar A and Aggarwal S. K. Saini L. M. and Kumar A. 2011). In the narrow speed range operations of SRIMD, slip power has a fraction of the motor power rating and so, converters power rating is small resulting decrease in size and cost of the SRIMD (Yang X. Xi L., Yang X. and Jiang J-g. 2008). At present the evolution in static converter/inverter technology is changing with a fastest pace and being utilized in the area of renewable energy sources (Rahi O. P. and Chandel A. K. 2015 and Rahi O.P. and Kumar A. 2016). The demerits of the conventional SPRS controlled SRIMDs are poor power factor, higher reactive power consumption of inverteter and poor quality of power supply (Shepherd W. and Stanway J. 1969).

To resolve the issues of power factor, reactive power and total harmonic distortion (THD) of supply, several publications (Sita Ram, Rahi O. P. and Sharma V. 2017) have been presented in the literature employing different approaches stressed on the performance improvement of SRIMDs. The various chopper configurations (Tunyasrirut S. Ngamwiwita J. Kinnares V. Furuya T. and Yama. motod Y. 2008, Tunyasrirut S. Kinnares V. and Ngamwiwit J. 2010, Tunyasrirut S. and Kinnares V. 2013, and Pardhi C. Yadavalli A. Sharma S. and Kumar G. A. 2014) have been implemented to enhance the power factor, efficiency and to reduce reactive power consumption of inverter, thereby, the THD of the supply. However the main contributions from the various researchers have given emphasis on buck or boost operation of chopper and inverter. The research in different chopper configurations (buck and buck-boost) is continuous with various power semiconductor technologies for inverter and chopper to enhance the power factor, efficiency and harmonic compensation of SRIMD (Sita Ram, Rahi O. P. and Sharma V. 2016, Sita Ram, Rahi O. P. Sharma V. Kumar P. Choudhary R. Vardhan G. and

Choudhary R. 2016, Sita Ram, Rahi O. P. Sharma V. and Murthy K. S. R. 2017, Bhardwaj S. R. Rahi O. P. and Sharma V. 2018]. The active and reactive power on the mains supply side can be controlled using PWMVSI with voltage and current control techniques in conjunction with buck-boost chopper in the DC link voltage circuit.

This paper presents the analysis of different performance characteristics of SPRS based SRIMD employing the buck-boost chopper and PWMVSI with current control technique. The performance characteristics include the reactive power, THD of power supply, power factor, and efficiency of SRIMD. The major focus of this research is to;

1. Propose the buck-boost chopper in the intermediate circuit to control the speed of induction motor.
2. Achieve the decoupled control as the proposed buck-boost chopper controls the speed of induction motor while the PWMVSI using current control technique controls the reactive power on AC side simultaneously, which in turn enhances the power factor of SRIMD.
3. Reduce the THD of the power supply current using sinusoidal PWMVSI with current control technique.

The Section II includes the System modeling simulation followed by the simulation results analysis in Section III and conclusions in Section IV.

II. System Structure and Modeling

In this section mathematical modeling of conventional SPRS along with proposed methodology has been illustrated.

2.1 Mathematical Modeling of Conventional SPRS

The schematic of conventional SPRS (Static- Kramer drive) shown in "Fig. 1" controls the speed of induction motor below synchronous speed. In this scheme, three-phase diode bridge rectifier converts the power recovered from the rotor circuit into DC power. The three-phase fully controlled line commutated inverter bridge, inverts this DC power into AC at the required frequency and fed it to back the three-phase AC source. The inverter output V_{d2} can be controlled by controlling the firing angle of the inverter bridge, thus, controls the feedback power as a result the rotor speed. The ripples in DC link current I_d can be minimized using DC link inductor L_d. The transformer matches the voltages V_{d2} and supply source considering an appropriate turn's ratio (Ram S. Rahi O.P. Sharma V. and Kumar . A. 2015).

The main equations governing the SPRS neglecting stator and rotor drops are given below

$$V_{d1} = \frac{3\sqrt{2}}{\pi} \times \frac{sV}{n} \Rightarrow 1.35 \times \frac{sV}{n} \quad (1)$$

$$V_{d2} = \frac{3\sqrt{2}}{\pi} \times \frac{V}{m} \cos\alpha \Rightarrow 1.35 \times \frac{V}{m} \cos\alpha \quad (2)$$

$$s = \frac{n}{m} |\cos\alpha| \quad (3)$$

The slip in terms of speed, DC link current, air gap power, and developed torque, respectively (Sita Ram, Rahi O. P. and Sharma V. 2016) can be written as following

$$s = \frac{\omega_{ms} - \omega_m}{\omega_{ms}} \quad (4)$$

$$I_d = \frac{V_{d1} + V_{d2}}{2(sR_1^{'} + R_2) + R_d} \quad (5)$$

$$P_g = 1.35 \frac{V}{n} \times I_d \quad (6)$$

$$T_d = \left(\frac{p}{2}\right) \frac{1.35V}{n \times \omega_{ms}} \times I_d \quad (7)$$

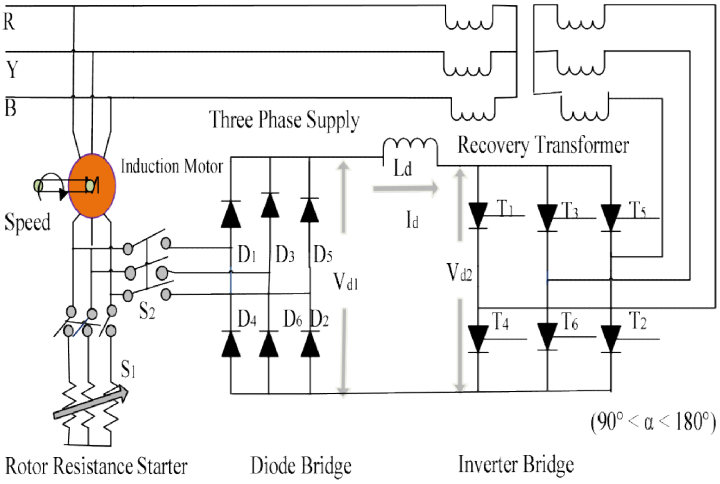

Fig. 1 Schematic of SPRS using line commutated inverter

where V_{d1} is the diode bridge output voltage, V_{d2} is the inverter bridge output voltage, α is the firing angle of inverter, n is the stator side to rotor side turns ratio of induction motor, m is a supply side to inverter side transformer turns ratio, s is the slip, V is the input voltage, I_d is DC link current, $R_1^{'}$ is stator resistance referred to rotor side, R_2 is rotor resistance, R_d is the resistance of DC link inductor, p is no of poles, P_g is power in the air gap, T_d is developed torque, P_m is mechanical power developed at the shaft, ω_{ms} and ω_m are the synchronous speed and rotor speed in rad/sec respectively. For the the secure commutation of thyristors highest value of α has been limited to 165°.

"Eq. 7" implies that the developed torque is directly proportional to DC link current and the magnitude of the current depends upon the difference between the V_{d1} and V_{d2}. The major weakness of conventional SPRS is the more reactive power drawn from the source for smaller firing angle of the inverter (higher speed) and returns less active power to the source, so it has lower power factor and higher THD of the supply (Sita Ram, Rahi O. P. Sharma V. Kumar P. Choudhary R. Vardhan G. and Choudhary R. 2016).

2.2 Proposed Methodology using PWMVSI with Current Control Technique

The schematic diagram of proposed system has been shown in "Fig. 2" consisting of an IGBT buck-boost chopper and diode bridge, DC link capacitors and PWMVSI using current control technique to eliminate the drawbacks of conventional SPRS. The complete circuit diagram of PWMVSI using current control technique is shown by "Fig. 3" and parameters of the system are given by table 2.1. The voltage V_{dc} is controlled at a constant value by the IGBT buck-boost chopper. Consequently variation of torque and speed is achieved by operation of the buck-boost chopper. Using the diode bridge connecting the rotor of the machine to the electronic circuit allows a simplified control system. The active and reactive power can be controlled by controlling the current of voltage source inverter side and AC line side connected with the reactor circuits (Pardhi C. Yadavalli A. Sharma S. and Kumar G. A. 2014). From "Fig. 3" the grid voltage can be written as given by "Eq. 8".

$$V_{grd} = V_{cnv} - V_L \quad (8)$$

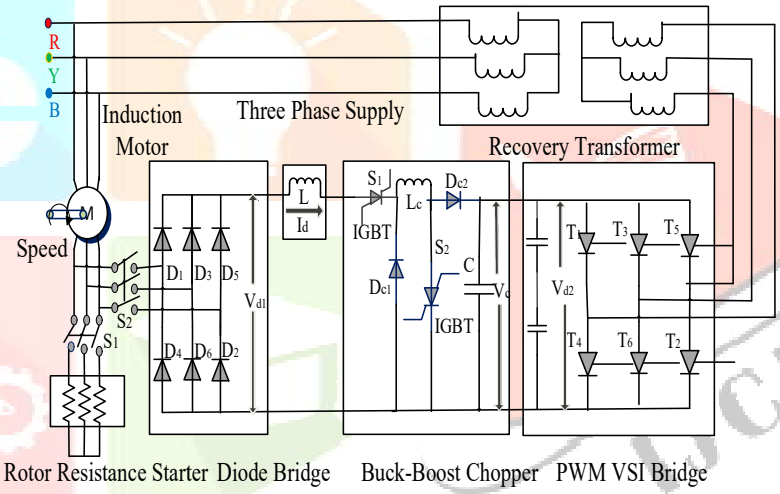

Fig. 2 Schematic diagram of SPRS employing buck-boost chopper and PWMVSI with current control technique

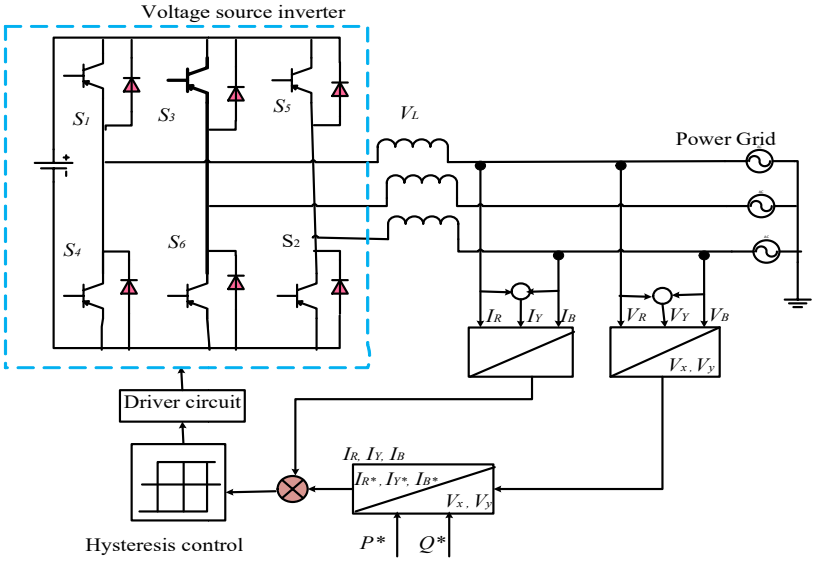

Fig. 3 Current Control Techniques for PWM VSI [10]

Table 2.1 System Parameters of SPRS

Parameter	Values	Parameter	Values
Rated power (P_{out})	2 hp	Moment of inertia (J)	0.2 Kg.m^2
Rated voltage (V)	415 V	Stator to rotor turns ratio (n)	5
Rated current (I_r)	3.6 A	Turns ratio of transformer (inverter to line side) (m)	0.2
Frequency (f)	50 Hz	Resistance of DC link inductor (R_d)	2 Ohm
Phases (p)	3	Inductance of DC link inductor (L_d)	0.025H
Pole pairs (p/2)	2	Inductance of buck-boost chopper (L_c)	0.005H
Stator resistance (R_1)	6 Ω	Capacitance of buck-boost chopper (C)	750μF
Stator leakage reactance (X_1)	7 Ω	Power rating of SCR/GTO/MOSFET/IGBT inverter (P_{inv})	1kVA
Rotor resistance (R_2)	5 Ω	Voltage (rms) rating of inverter (V_{d2})	80V
Rotor leakage reactance (X_2)	7 Ω	Ratings of buck-boost chopper (P_{ch}/ V_c)	1kVA/(4-80V)
Magnetizing reactance (X_m)	147 Ω	Switching frequency of inverter and chopper	1kHz

The active and reactive power flow between grid side and converter side can be written as

$$P = \frac{V_{grd}^2}{\omega_L}\left(\frac{V_{cnv}}{V_{grd}}\sin\theta\right) \tag{9}$$

$$Q = \frac{V_{grd}^2}{\omega_L}\left(1-\frac{V_{cnv}}{V_{grd}}\cos\theta\right) \tag{10}$$

where apparent power is given by

$$S = v \times i^* = P + jQ \tag{11}$$

The instantaneous real and imaginary power is part to the instantaneous complex power defined as (Tunyasrirut S. and Kinnares V. 2013)

$$S = \left(v_x \times i_x + v_y \times i_y\right) + j\left(v_y \times i_x + v_x \times i_y\right) \tag{12}$$

From the transformation matrixes, the Clark transformation and its inverse transformation become

$$\begin{bmatrix} v_x \\ v_y \end{bmatrix} = \begin{bmatrix} 1 & -1/2 & -1/2 \\ 0 & \sqrt{3}/2 & -\sqrt{3}/2 \end{bmatrix} \begin{bmatrix} v_a \\ v_b \\ v_c \end{bmatrix} \tag{13}$$

The instantaneous power of the *p-q* theory

$$\begin{bmatrix} P \\ Q \end{bmatrix} = \begin{bmatrix} v_x & v_y \\ -v_y & v_x \end{bmatrix} \begin{bmatrix} i_x \\ i_y \end{bmatrix} \tag{14}$$

In the following explanation, the currents will be set as functions of voltage and the real and imaginary power P and Q . In the $p\ q$ theory, it is possible to write

$$\begin{bmatrix} i_x \\ i_y \end{bmatrix} = \frac{1}{v_x^2 + v_y^2} \begin{bmatrix} v_x & v_y \\ v_y & -v_x \end{bmatrix} \begin{bmatrix} P \\ Q \end{bmatrix} \tag{15}$$

The inverse Clark transformation can be decomposed into the sum of two terms, as follows (Tunyasrirut S. and Kinnares V. 2013)

$$\begin{bmatrix} i_a^* \\ i_b^* \\ i_c^* \end{bmatrix} = \begin{bmatrix} 1 & 0 \\ -1/2 & \sqrt{3}/2 \\ -1/2 & -\sqrt{3}/2 \end{bmatrix} \begin{bmatrix} i_x \\ i_y \end{bmatrix} \tag{16}$$

2.3 Mathematical Model of SPRS using Buck-Boost Chopper

The equations for output voltage of inverter and slip using buck-boost chopper are expressed as below, where δ represents the duty ratio of the chopper.

$$V_{d2} = \frac{3\sqrt{2}}{\pi}\left(\frac{\delta}{1-\delta}\right)\frac{V}{m}cos\alpha \Rightarrow 1.35\left(\frac{\delta}{1-\delta}\right)\frac{V}{m}cos\alpha \tag{17}$$

$$s = \frac{n}{m}\left(\frac{\delta}{1-\delta}\right)|cos\alpha| \tag{18}$$

Duty ratio of the chopper can be controlled from 0 to1 and so slip can be controlled by proper choice of α or δ to acquire the required speed (Sita Ram, Rahi O. P. Sharma V. and Murthy K. S. R. 2017).

The inverter recovered power, power factor, air gap power, and developed electromagnetic torque can be derived using DC equivalent circuit (Bhardwaj S. R. Rahi O. P. and Sharma V. 2018) given by following equations.

$$cos\phi = \frac{(P_s - P_{rec})}{\sqrt{(P_s - P_{rec})^2 + (Q_s + Q_{rec})^2 + P_h^2}} \tag{19}$$

$$P_{rec} = 1.35V\left(\frac{\delta}{1-\delta}\right)cos\alpha \times I_d$$

$$\Rightarrow 1.35V\left(\frac{\delta}{1-\delta}\right)\cos\alpha \times \frac{1.35V\left\{\frac{s}{n} - \left(\delta/1-\delta\right)\cos\alpha/m\right\}}{\left[2R_1' + \left\{3(X_1' + X_2)/\pi\right\}\right]s + R_2 + R_d} \tag{20}$$

$$Q_{rec} = 1.35V\left(\frac{\delta}{1-\delta}\right)sin\alpha \times I_d$$

$$\Rightarrow 1.35V_{d2}\left(\frac{\delta}{1-\delta}\right)sin\alpha \times \frac{1.35V\left\{\frac{s}{n} - \left(\delta/1-\delta\right)\cos\alpha/m\right\}}{\left[2R_1' + \left\{3(X_1' + X_2)/\pi\right\}\right]s + R_2 + R_d} \tag{21}$$

where

$$R_{dc} = \left\{2R_1' + \frac{3(X_1' + X_2)}{\pi}\right\}s + R_2 + R_d \tag{22}$$

$$I_d = \frac{V_{d1} - V_{d2}}{R_{dc}} \Rightarrow \frac{1.35V\left\{\frac{s}{n} - \left(\delta/1-\delta\right)\cos\alpha/m\right\}}{\left[2R_1' + \left\{3(X_1' + X_2)/\pi\right\}\right]s + R_2 + R_d} \tag{23}$$

$$P_g = \frac{|V_{d2}|I_d}{s}$$

$$\Rightarrow \frac{\left\{1.35\left(\frac{\delta}{1-\delta}\right)\frac{V}{m}\cos\alpha\right\} \times \frac{1.35V\left\{\frac{s}{n} - \left(\delta/1-\delta\right)\cos\alpha/m\right\}}{\left[2R_1' + \left\{3(X_1' + X_2)/\pi\right\}\right]s + R_2 + R_d}}{s} \tag{24}$$

$$T_d = \frac{P_g}{\omega_{ms}} \Rightarrow \frac{|V_{d2}|I_d}{s\omega_{ms}}$$

$$\Rightarrow \frac{\left\{1.35\left(\frac{\delta}{1-\delta}\right)\frac{V}{m}\cos\alpha\right\} \times \frac{1.35V\left\{\frac{s}{n} - \left(\frac{\delta}{1-\delta}\right)\frac{\cos\alpha}{m}\right\}}{\left\{2R_1' + \frac{3(X_1' + X_2)}{\pi}\right\}s + R_2 + R_d}}{s\omega_{ms}} \tag{25}$$

where P_{rec} and Q_{rec} are the inverter recovered active and reactive powers, P_g and T_d are the air gap power and developed electromagnetic torque using buck-boost chopper respectively. P_s, Q_s are the active power active and reactive power drawn from the source, P_h is the harmonic power loss and can be expressed utilizing AC equivalent circuit of SPRS given by following equs. (Bhardwaj S. R. Rahi O. P. and Sharma V. 2018)

$$P_s = 3 \times V_{ph} \times I_r \cos\phi_s \tag{26}$$

$$Q_s = 3 \times V_{ph} \times I_r \sin\phi_s \tag{27}$$

$$P_h = \frac{V_h}{\sqrt{R^2 + X^2}} \tag{28}$$

where V_{ph} is the stator phase voltage and I_r and φ_s are the rotor current and the phase angle between stator voltage and rotor current, , $R = R_1 + \left(R_{d1} + \frac{R_{d2}}{s}\right)n^2$ and $X = X_1 + X_2 \times n^2$, R_1 and X_1 are the stator resistance and reactance, respectively.

Using “Eq. 23” Eq. 24” “Eq. (29)” and “Eq. 30” active and reactive power supplied by the source can be expressed as

$$P_s - P_{rec} \Rightarrow V_{ph} \times I_r \cos\phi_s - 1.35V\left(\frac{\delta}{1-\delta}\right)cos\alpha \times I_d \tag{29}$$

$$Q_s + Q_{rec} \Rightarrow 3 \times V_{ph} \times I_r \sin\phi_s + 1.35V\left(\frac{\delta}{1-\delta}\right) sin\alpha \times I_d \quad (30)$$

Thus net input power supplied to the SRIM is given by equation below

$$P_i = \sqrt{\left(P_s - P_{res}\right)^2 + \left(Q_s + Q_{rec}\right)^2 + P_h^2} \quad (31)$$

"Eq. 21" specified that the reactive power can be controlled by changing the duty cycle of chopper and keeping firing angle of inverter fixed; so, improve the power factor as depicted by "Eq. 19". "Eq. 31" implies that increase in feedback active power and decrease in the reactive power decreases the net input power drawn from the source leading to increase in efficiency of the SRIMD.

2.4 Buck-Boost Chopper Configuration

The different chopper techniques depicted in the literature are buck or boost, and buck-boost. However the buck or boost chopper have restrictions on minimum turn-on power (Pardhi C. Yadavalli A. Sharma S. and Kumar G. A. 2014) or voltage stability (Prasannakumar K. and Das B. B. 2014). The buck-boost chopper overcomes the problems associated with buck or boost chopper and can be operated in a buck, boost, and buck-boost mode depending upon the duty.

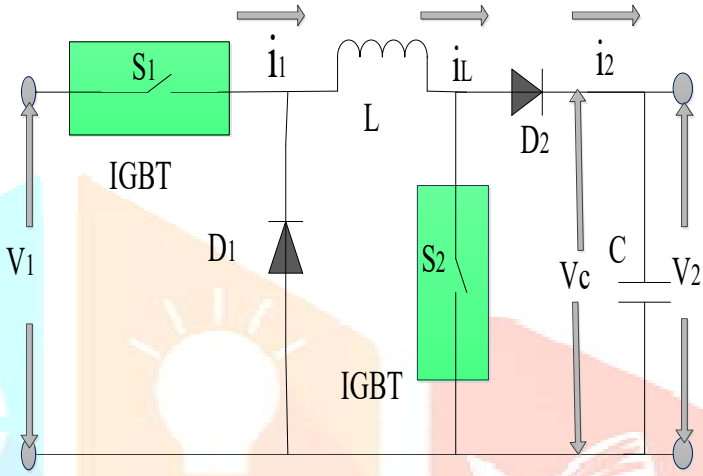

Fig. 4 Schematic diagram of buck-boost chopper

"Fig. 4" shows the schematic of buck-boost chopper employing IGBT power electronic devices. The designing of the buck-boost chopper depends upon the parameter i.e. minimum input voltage $V_{i\,min}$, maximum input voltage $V_{i\,max}$, V_o nominal output voltage and integrated circuit used to manufacture the buck-boost chopper (Green M. 2012). The inductor L shown in "Fig. 4" is required to have a current magnitude higher than the largest value of current for the buck and boost mode of the chopper operation owing to the increase in peak current with the decrease in inductance. The capacitor C maintain the constant voltage or limit the ripples of the voltage and supplies the total output current during the switch on state position. The switch S_1 and S_2 controls the energy from the input source to the output voltage (side). The diode D_1 and D_2 conducts when the switches S_1 and S_2 are off and allow the inductor current to pass through. The voltage rating of the switch and diode depends upon the maximum value of voltage difference between the input and output voltages and transient spikes. Usually the maximum value of inductor output current is taken as twice of the switching current (Rogers E. 1999).

III. Simulation Results

The simulation models of SPRS using chopper and PWMVSI with current control technique have been developed in MATLAB R2013a using a *2 hp*, *415V*, *50Hz*, *1430 rpm* SRIM. A load torque of *8 Nm* has been applied to the motor. The speed, rms value of current and power factor have been measured using Fourier blocks. The active and reactive powers have been measured using discrete blocks. MATLAB inbuilt tool Graphical User Interface has been used for the THD or Fast Fourier Transform analysis. The different characteristics have been plotted and illustrated in this section. The efficiency (%) of the induction motor have been computed as

$$\eta = \frac{P_{out}}{P_{in} - P_{fb}} \times 100 \quad (32)$$

where P_{in} and P_{fb} in Watts are meseared input and feedback powers of the induction motor by the discrete blocks and P_{out} in Watts is the the mechanical power output at the shaft [12].

3.1 Results using Line Commutated SCR Inverter without chopper

This section illustrates the simulation results of conventional SPRS using line commutated SCR inverter without chopper. In this case the rotor speed of induction motor is controlled by varying the firing angle of inverter bridge. The scope data recorded from the Simulink model of SPRS without chopper have been shown in "Figs. (5-7)" for a speed of *1200 rpm* or slip of *0.2*. "Fig. 5" presents the waveforms of (a) source current, (b) source voltage and (c) stator current measured, whereas the "Fig. 6" the waveforms of (a) DC link current, (b) inverter voltage, (c) inverter current and (d) inverter voltage respectively. "Fig. 7" shows the FFT window of SPRS at speed of *1200 rpm* or slip of *0.2* representing the THD of supply current as *84.54%.* "Figs. (8and 9)" show the variations of the speed and feedback power with firing angle of inverter, where the symbols N_r and P_{fb} represents the rotor speed of induction motor and the feedback active power sent back to the supply source respectively.

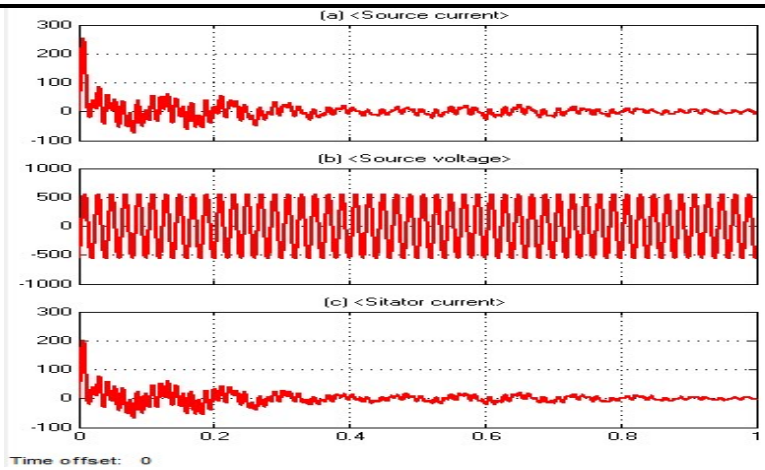

Fig. 5 Waveforms of (a) source current, (b) inverter voltage and (c) stator current

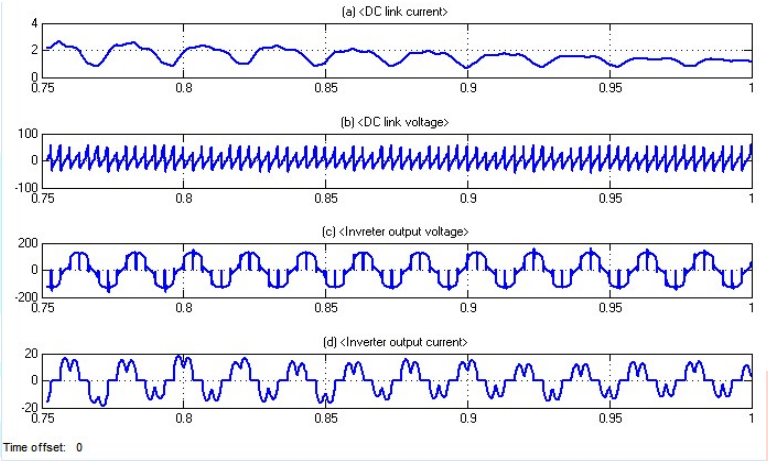

Fig. 6 Waveforms of (a) DC link current, (b) DC link voltage, (c) inverter current, and (d) inverter voltage

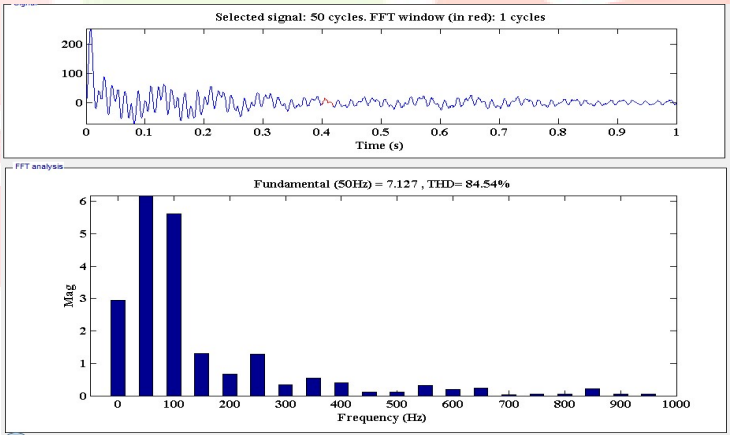

Fig. 7 FFT window SPRS without chopper

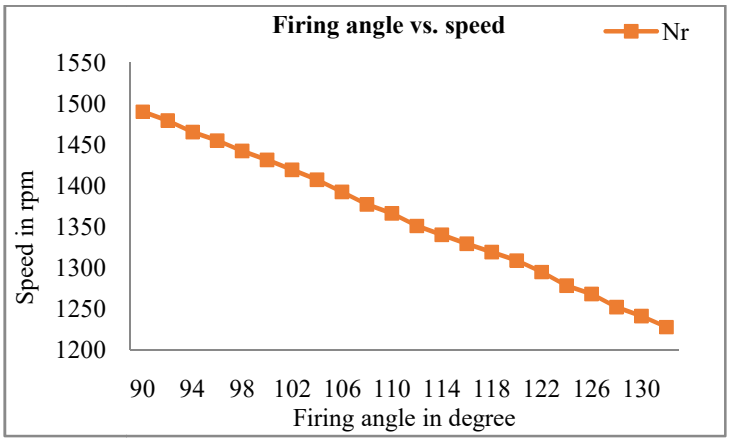

Fig. 8 Graph of firing angle vs. rotor speed using SCR inverter without chopper

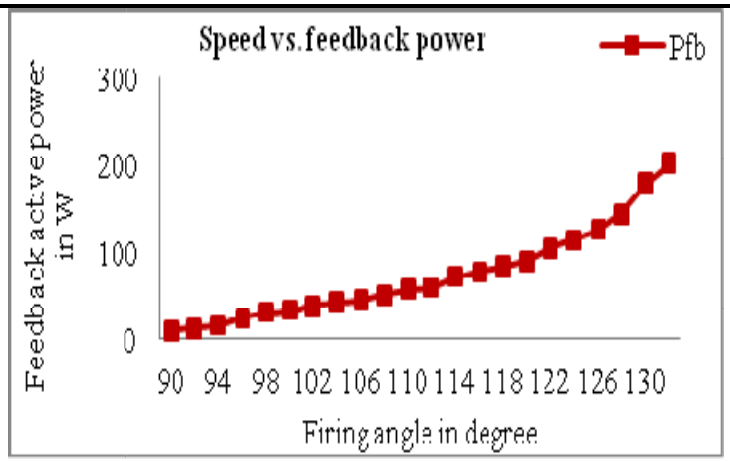

Fig. 9 Graph of firing angle vs. feedback power using SCR inverter without chopper

From the "Fig. 8", it is seen that as the firing angle increases the rotor speed decrease and vice-versa, because with the increase in firing angle, the inverter output voltage V_{d2} increases leading to increase in the feedback power shown by "Fig. 9". As the feedback power increases the equivalent electrical or mechanical power developed at the shaft decreases, causing reduction in rotor speed for the constant load.

3.2 Results using Buck-Boost Chopper and PWMVSI with Current Control Technique

This sub-section includes the simulation results of SPRS employing the buck-boost chopper and PWMVSI with current control technique. In the simulation model, the modulation index of the PWMVSI is kept fixed value and the rotor speed is controlled by varying the duty ratio of the buck-boost chopper from *80%-30%* at an interval of *5%*. The different waveforms measured form the Simulink scope using chopper and PWMVSI with current control technique have been shown in "Figs. (10-12)" for a speed of *1200 rpm* or slip of *0.2*.

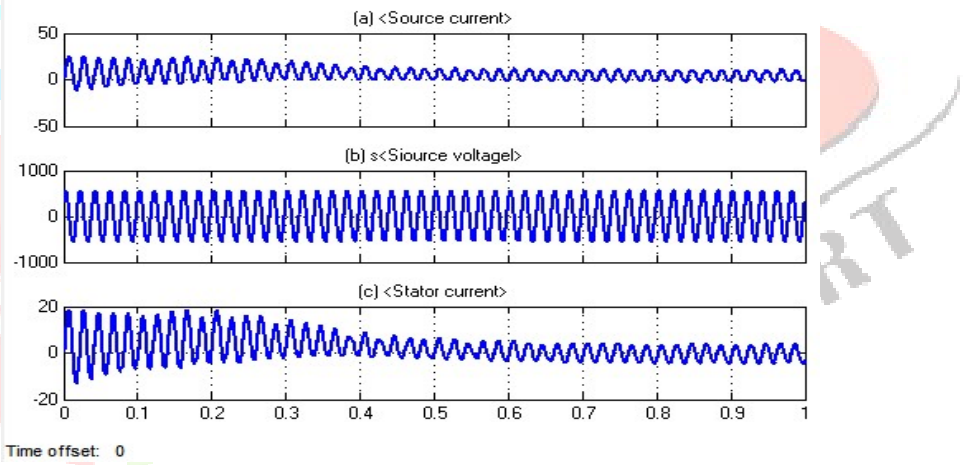

Fig. 10 Waveforms of source current and voltage and stator current

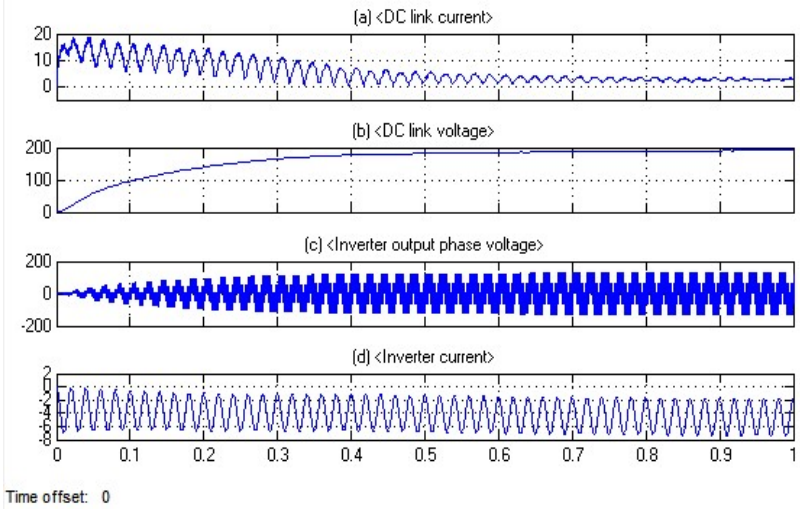

Fig. 11 Waveforms of (a) DC link current and (b) DC link phase voltage, (c) inverter current and (d) inverter phase voltage

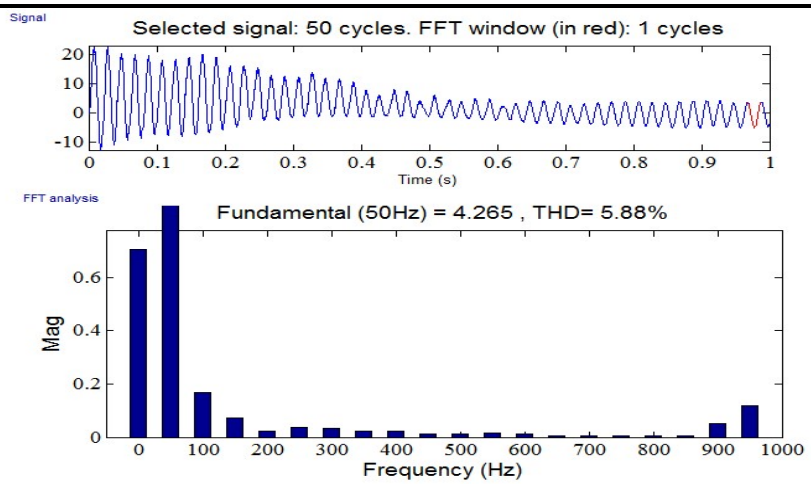

Fig. 12 FFT window SPRS with chopper and PWMVSI using voltage control technique

Here in this case "Fig. 10" presented the waveforms of (a) source current, (b) source voltage and (c) stator current, while the "Fig. 11", the waveforms of (a) DC link current, (b) DC link voltage (c) inverter current I_v, and (d) inverter pase voltage E_{ph} respectively. "Fig. 12" illustrates the harmonic spectrum of SPRS observed from the FFT window at speed of *1200 rpm* or slip of *0.2* representing the THD of supply current as *5.88%.* From the "Figs. (5 and 10)" it has been observed that the distortion of the source current, source voltage, and stator are less in the later case. "Figs. (6 and 11)" revealed that the DC link current, DC link voltage are more smooth in the later case. "Fig. (7 and 12)" demonstrated that the utilization of chopper and PWMVSI with current control technique has reduced the THD of the supply current from *84.54%* to *4.31%* at a speed of *1200 rpm* or slip of *0.2*. Hence improve the quality of power suply. "Figs. (13 and 14)" shows the variation in speed and feedback power relative to duty ratio, where $N_{r\text{-}cc}$ and $P_{fb\text{-}cc}$ represents the rotor speed and feedback active power respectively, using buck- boost chopper and PWMVSI with current control technique. The "Fig. 13" shows that the rotor speed decreases with the decrease in duty ratio of the chopper. The output of the buck-boost chopper is the function of switch off time as during off time period the energy is delivered to output or load side.

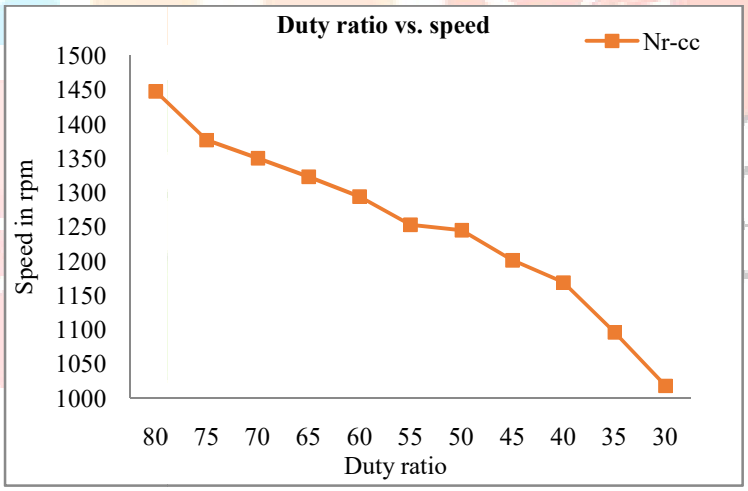

Fig. 13 Graph of duty ratio vs. speed using PWMVSI with current control technique

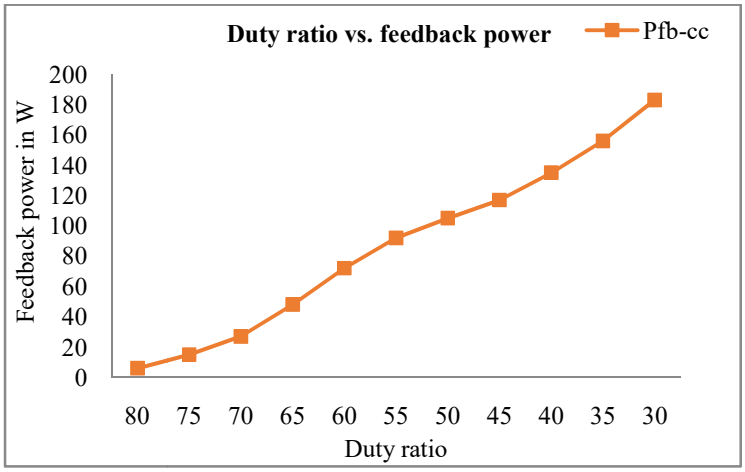

Fig. 14 Graph of duty ratio vs. feedback power using PWMVSI with current control technique

To decrease the duty ratio of chopper, the switch on time of chopper is decreased which in turn increases the switch off time for constant frequency operation of the chopper, consequently, increases the output power of the chopper. This increase in output of chopper increases the feedback power of the SPRS as depicted in "Fig. 14" and correspondingly decreases the rotor speed.

3.3 Comparative Results without and with Buck-Boost Chopper and PWMVSI with Current Control Technique

"Figs. (15 and 16)" shows the comparative the variations of source active and reactive powers with speed respectively, using SCR inverter without chopper and buck-boost chopper and PWMVSI using current control technique. Where the P_{in} and Q_{in} represents the source active and reactive powers using SCR inverter without chopper and the $P_{in\text{-}cc}$ and $Q_{in\text{-}cc}$ indicate the source active and reactive powers drawn from the source by the PWMVSI with control technique respectively. "Fig. 15" shows that the source active power decreases with the decrease in rotor speed in both the cases because decrease in speed increases the feedback active power sent back to the supply source. The net input active power taken by SRIM from the source decreases with the increase in feedback active power because in case of SPRS the net input active power drawn from the source is the difference of actual input active power to be drawn from the source minus feedback active power. This decrease in source active power drawn from the source improves the efficiency of SRIM. "Fig. 16" indicates that the source reactive power drawn from the source increases with the increase in firing angle, which in turn increases the THD of supply source and reduces the source power factor revealed by "Eq. 21".

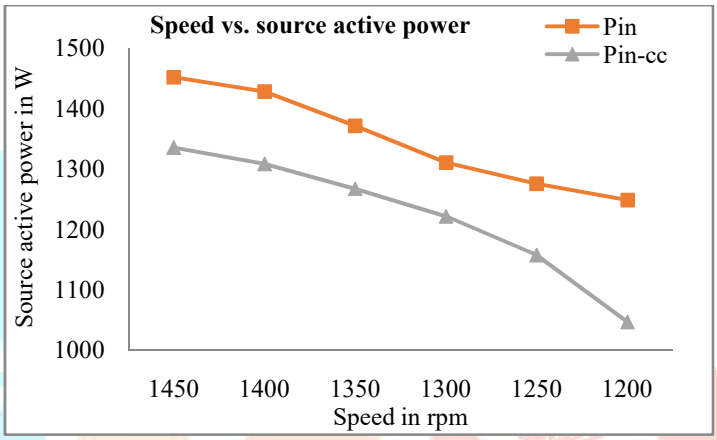

Fig. 15 Comparative graph of speed vs. source active power

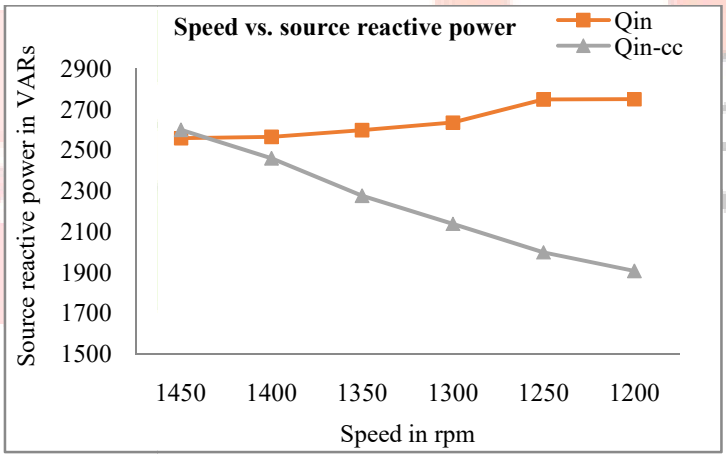

Fig. 16 Comparative graph of speed vs. source reactive power

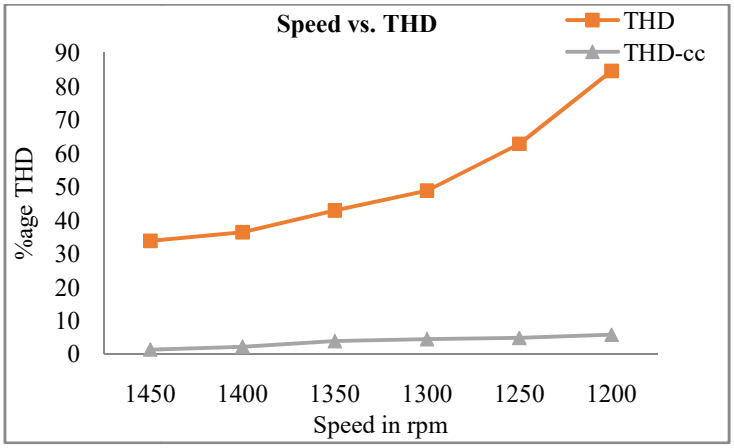

Fig. 17 Comparative graph of speed vs. THD

However the source reactive power decreases with the decrease in speed in case of PWMVSI with current control technique leading to reduce the THD of supply. Table 3.1 and "Figs. (17-19)" have presented the comparative results of speed vs. power factor, efficiency, and THD of supply represented by THD_{-cc}, $cos\varphi_{s-cc}$, and η_{-cc}, respectively using SPRS without chopper as well as chopper and PWMVSI with current control technique. The results have been compared on the basis of equal speed range, frequency, and load torque of SRIMD. "Fig. 17" illustrates the comparative graph of speed and THD of supply using both the methodologies with the average values of *51.54%* and *3.80%* respectively depicted in table 3.1. From table 3.1 and "Fig. 17" it has been investigated that the THD of supply increases with the decrease in rotor speed for both the cases yet, the increase in THD has less using chopper and PWMVSI with current control technique therefore has better quality of power supply. The comparative graph of speed and power factor for both the methodologies has been shown in "Fig. 18" which indicates the decrease in source power factor corresponding to rotor speed. However the decrease in power factor with speed is less using chopper and PWMVSI with current control technique. The average values of power factor for rotor speed control up to *1200 rpm* or slip of *0.2* for both the methodologies has been found to be *0.67* and *0.91* respectively depicted in table 3.1.

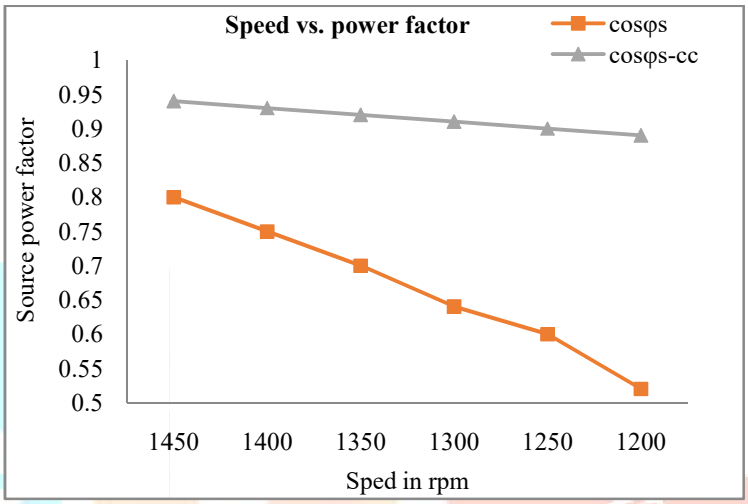

Fig. 18 Comparative graph of slip vs. source power factor

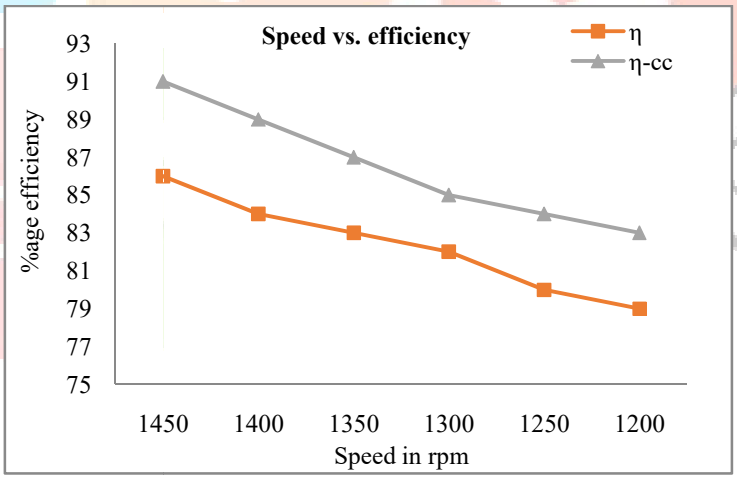

Fig. 19 Comparative graph of speed vs. efficiency

Table 3.1 Comparative results of speed vs. THD of supply, source power factor, and efficiency

S. No.	Rotor speed (rpm)	%age THD		Source power factor		%age efficiency	
	N_r	THD	THD_{-vc}	$Cos\varphi_s$	$Cos\varphi_{s-vc}$	η	η_{-vc}
1	1450	33.81	1.39	0.8	0.94	86	91
2	1400	36.41	2.22	0.75	0.93	84	89
3	1350	42.92	3.93	0.7	0.92	83	87
4	1300	48.79	4.51	0.64	0.91	82	85
5	1250	62.79	4.86	0.6	0.90	80	84
6	1200	84.54	5.88	0.54	0.89	79	83
Average		51.54	3.80	0.67	0.91	82	86.5

Therefore, the chopper and PWMVSI with current control technique have the higher average power factor compared to the SCR inverter control without chopper. The comparative graph of speed vs. efficiency for both cases has been shows in "Fig. 19". It has been observed from the table 3.1 and "Fig. 19" that the efficiency decreases corresponding to speed and the average values of efficiency recorded as *82%* and *86.5%* respectively. The decrease in efficiency in the later case is less compared to former because of lesser conduction and switching losses in the IGBT semiconductor devices. Therefore the efficiency of SRIMD is more using chopper and PWMVSI with voltage control technique..

IV. CONCLUSIONS

This paper has investigated the performance characteristics of SPRS based SRIMD employing buck-boost chopper and PWMVSI with current control technique. The performance characteristics have been considered for analysis i.e. THD of supply, power factor and efficiency of SRIMD. The comparative analysis of simulation results have shown that the chopper and PWMVSI with current control technique have reduced the average THD of supply from 51.54% to 3.80% and improved the average source power factor from 0.67 to 0.91 as well as average efficiency from 82% to 86.5%, respectively for a speed up to 1200 rpm or slip of 0.2. From these results it has been concluded that the SPRS using buck-boost chopper and PWMVSI with current control technique reduced the reactive power consumption of inverter, thereby, the THD of supply and enhances the power factor as well as efficiency of SRIMD compared to SPRS without chopper.

REFERENCES

[1] Lavi A and Polge R. J. 1966. Induction Motor Speed Control with Static Inverter in the Rotor. IEEE Transaction on Power Apparatus and System, 85:76-84.

[2] Kumar A, Aggarwal S. K. Saini L. M. and Kumar A. 2011.Performance Analysis of A Microcontroller Based Slip Power Recovery Drive. International Journal of Engineering Science and Technology, 3(3):25-35.

[3] Yang X. Xi L., Yang X. and Jiang J-g. 2008. Research on the Application Of PFC Technology in Cascade Speed Control System. IEEE 3rd Conference on Industrial Electronics and Applications (ICIEA): 1964-1969.

[4] Rahi O. P. and Chandel A. K. 2015. Refurbishment and Uprating of Hydro Power Plants-A Literature Review. Renewable and Sustainable Energy Reviews, 48:726-737.

[5] Rahi O.P. and Kumar A. 2016. Economic Analysis for Refurbishment and Uprating of Hydro Power Plants. Renewable Energy, 86: 1197-1204.

[6] Shepherd W. and Stanway J. 1969. Slip Power Recovery In an Induction Motor by the Use of A Thyristor Inverter. IEEE Transaction on Industry and General Applications, 5(1):74-82.

[7] Sita Ram, Rahi O. P. and Sharma V. 2017. A Comprehensive Literature Review on Slip Power Recovery Drives. Renewable and Sustainable Energy Reviews, 73: 922-934.

[8] Tunyasrirut S. Ngamwiwita J. Kinnares V. Furuya T. and Yama. motod Y. 2008. A DSP-Based Modified Slip Energy Recovery Drive Using a 12-Pulse Converter and Shunt Chopper for a Speed Control System of a Wound Rotor Induction Motor. Electric Power System Research, 78(5): 861-872.

[9] Tunyasrirut S. Kinnares V. and Ngamwiwit J. 2010. Performance Improvement of Slip Energy Recovery System by a Voltage Controlled Technique. Renewable Energy, 35:2235-2242.

[10] Tunyasrirut S. and Kinnares V. 2013. Speed and Power Control of a Slip Energy Recovery Drive using Voltage-Source PWM Converter with Current Controlled Technique. 10th Eco-Energy and Materials Science and Engineering Symposium, 326-340.

[11] Pardhi C. Yadavalli A. Sharma S. and Kumar G. A. 2014. A Study of Slip-Power Recovery Schemes with A Buck DC Voltage Intermediate Circuit and Reduced Harmonics on the Mains by various PWM Techniques. International Conference on Computation of Power, Energy Information and Communucation (ICCPEIC-2014).495-499.

[12] Ram S. Rahi O.P. Sharma V. and Kumar. A. 2015. Performance Analysis of Slip Power Recovery Scheme Employing Two Inverter Topologies. Michal Faraday IET International Summit (MFIIS), Kolkata, India, 356-361.

[13] Sita Ram, Rahi O. P. and Sharma V. 2016. Analysis of Induction Motor Drive using Buck-Boost Controlled Slip Power Recovery Scheme. IEEE International Conference on Power Electronics, Intelligent. Control and Energy Systems, Delhi Technical University Delhi, 1-6.

[14] Sita Ram, Rahi O. P. Sharma V. Kumar P. Choudhary R. Vardhan G. and Choudhary R. 2016. Reactive Power Control Of Induction Motor Drive Using Chopper Operated Slip Power Recovery Scheme. Proceedings of IEEE 7th Power India International Conference (PIICON), Govt. Engineering College Bikaner Rajasthan.

[15] Sita Ram, Rahi O. P. Sharma V. and Murthy K. S. R. 2017. Investigations in to Induction Motor Drive using Slip Power Recovery Scheme with GTO Inverter and Chopper. 14th IEEE India Council International Conference (INDICON) Indian Institute of Technology Roorkee, India, 1-6.

[16] Bhardwaj S. R. Rahi O. P. and Sharma V. 2018. Comparative Analysis of Induction Motor Drive with Chopper Controlled SPRS Employing Various Inverter Configurations. IETE Journal of Research, http://dx.doi.org/10.1080/03772063. 2018.1431065.

[17] Prasannakumar K. and Das B. B. 2014. Digital Combination Of Buck And Boost Converters To Control A Positive BuckBoost Converter And Improve Output Transients. International Journal and Magazine of Engineering, Technology, Management and Research, 1(9):50-56,.

[18] Green M. 2012. Design Calculation for Buck-Boost Converters. Application Report, Texas Instruments Literature Number SLVA535A.

[19] Rogers E. 1999. Understanding Buck-Boost Power Stages in Switch Mode Power Supplies. Application Report, Texas Instruments Literature Number SLVA059.